arXiv:hep-ph/0309043 v1 4 Sep 2003

DESY 03-118

QCD Corrections to $\gamma\gamma \to ZZ$ at Small Scattering Angles

Grigorios Chachamis[(a)1] and Krisztián Peters[(a)2]

[(a)] *II. Institut für Theoretische Physik, Universität Hamburg, Luruper Chaussee 149, D-22761 Hamburg*

Abstract

QCD corrections to the electroweak cross section of $\gamma\gamma \to ZZ$ at high energies and small scattering angles have been calculated. The dominant contributions are due to t-channel gluon exchange, i.e. photons dissociate into quark-antiquark pairs giving rise to two colour dipoles which interact through gluons. Corrections resulting from the leading log BFKL amplitude are of the order of a few percent close to the forward region already at the 1 TeV energy range and are rising with the scattering energy. We also considered the helicity non-conserving cases in which the QCD corrections in comparison to the electroweak part of the amplitude strongly grow with energy. The helicity non-conserving scattering process is of particular interest since it is sensitive to the Higgs sector.

[1] email: grigorios.chachamis@desy.de
[2] email: krisztian.peters@desy.de

1. The correct extension of the Standard Model (SM) and the determination of the electroweak symmetry breaking mechanism are one of the basic questions which have to be answered in the nearest future. Experimentally, we expect the first data and insights concerning these questions after the run of the Large Hadron Collider (LHC). Complementary, high precision measurements will come from the Next Linear Collider (NLC) e.g. TESLA, opperating in the energy regime up to 1 TeV and providing a very clean enviroment. In addition one may have the capability of running the NLC in a $\gamma\gamma$ collision mode via Compton backscattering of laser photons off the linear collider electrons. Apart from the advantage of the higher luminosity, the energy of the initial photons can be determined more accurately than the energy of photons radiated in the e^+e^- collider mode. One of the important processes one will consider at the NLC is the production of vector bosons such as $\gamma\gamma \to ZZ$ [1].

Concerning the search of physics beyond the Standard Model, the fact that the first perturbative contribution starts at one loop makes the process $\gamma\gamma \to ZZ$ sensitive to a number of investigations. One is the search for the existence of anomalous triple and quartic vector boson couplings [2] or vector boson Higgs couplings [3]. The natural order of magnitude of these couplings [4] is small, so one needs to know the SM cross sections with a precision better than 1%. In order to get a detailed understanding of the spin structure of anomalous couplings, it is important to investigate the different helicity states of the outgoing Z bosons. Because of the absence of the tree level contribution, this process is sensitive also to particles and new physics phenomena contributing through radiative corrections [5]. This leads to a method independent of and complementary to the direct production of new particles. Again, high precision of the Standard Model cross section is needed. In addition, the detection of CP violating phases [6] or effects due to the exchange of Kaluza-Klein gravitons in large extra dimension scenarios [7] have been discussed.

Another motivation to study the process $\gamma\gamma \to ZZ$ is its sensitivity to the Higgs sector. At high energies the biggest contribution to the cross section comes from the production of transverse polarised Z bosons in the kinematical limit of small scattering angles (helicity conserving channel). The dominant contribution to the scattering amplitudes is due to W loops and grows proportional to the scattering energy s. Compared to these leading contributions, the diagrams containing the Higgs contribution are supressed by s^2. In contrast to this, in the production of longitudinal Z bosons the Higgs plays a crucial role. In this channel, both the Higgs contribution and the W loop are constant in s (up to powers of logarithms). For large Higgs masses the s-channel Higgs exchange in the scattering amplitude of $\gamma\gamma \to Z_L Z_L$ violates partial-wave unitarity [9,8] and makes this helicity non-conserving case sensitive to the Higgs sector. Therefore we need to know the SM cross section with a high precision in order to disentangle different symmetry breaking scenarios.

In summary, the process $\gamma\gamma \to ZZ$ is an important tool to probe physics beyond the SM. In order to see deviations, high precision is needed, both on the experimental and on the theoretical side. A calculation at the lowest available order may not be accurate enough. Since the cross section gains its biggest contribution from small scattering angles, it is natural to ask whether QCD corrections could play a role in this kinematical regime. At high energies the most dominant corrections arise when the vector bosons fluctuate into quark-antiquark pairs, described by the boson impact factors, and these dipoles interact through gluon exchanges. At higher orders in α_s large logarithms in s emerge, leading to

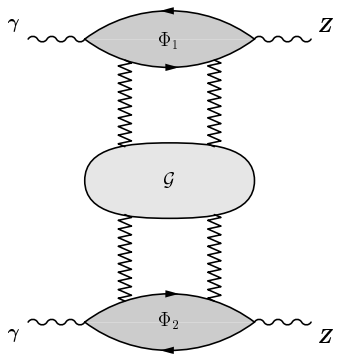

Figure 1: The BFKL exchange in the $\gamma\gamma \to ZZ$ elastic cross section.

QCD corrections rising with the scattering energy. At very high energies these corrections will be large and cannot be neglected.

In this letter we adress the question whether in the energy region of the NLC QCD corrections need to be taken into account. For this purpose we compute the differential cross section both for the electroweak and the QCD parts. For the helicity conserving channel the QCD corrections have been studied recently [10]. In this letter we extend our analysis to the helicity non-conserving channel. The electroweak part was computed first in [1], but for our purposes we had to repeat the full one loop calculation. For the helicity conserving case it turns out that QCD corrections in the region of about 1 TeV are at the percent level and grow moderately with energy. For the helicity breaking channel the QCD corrections to the differential cross section, at about 1 TeV, are of the same order, but they grow much faster with increasing energy.

2. The differential cross section including the QCD corrections reads:

$$\frac{d\sigma}{dp_T^2} = \frac{1}{16\pi s^2}|A_{EW} + A_{QCD}|^2\,, \tag{1}$$

with p_T being the exchanged transverse momenta, whereas the corrections to the pure electroweak amplitude are dictated by the interference term. The calculation was performed in the Feynman gauge.

The electroweak part of the amplitude was first computed in a full one loop calculation by Jikia [1] for Higgs masses over 300 GeV. In order to compute the above mentioned interference term, the results of [1] have been reproduced, however we used in this letter an up to date value of the top quark mass and a Higgs mass of $m_H = 115$ GeV. We adopted the definition of momenta and polarisation vectors from [11]. The Feynman diagrams were generated with *FeynArts* [12] and the resulting amplitudes were algebraicaly simplified using *FormCalc* [11]. To evaluate the one-loop integrals the package *LoopTools* [11, 13] was used. At small scattering angles the main contribution to the amplitude comes from the bosonic loop of the helicity conserving channel. These amplitudes are mainly imaginary and proportional to s in this kinematical limit, in agreement with the calculation of [10] where a high energy approximation was used. For the helicity-flip

channels no contributions proportional to s survive, thus these amplitudes are supressed by one power of s compared to the helicity conserving cases. If one of the Z bosons has transverse and the other longitudinal polarisation, the amplitude is vanishing at the forward point ($p_T = 0$) due to angular momentum conservation.

The QCD part of the amplitude was calculated recently in [10], where the reader will find analytic expressions for A_{QCD}. In the small angle region these emerge when vector bosons fluctuate into a quark-antiquark pair and these dipoles interact through gluons. At the lowest order, when two gluons are exchanged in the t-channel, one obtains a contribution proportional to the scattering energy for both, the helicity conserving and helicity flip amplitudes. The radiation of more gluons enhances the cross section, since this higher order corrections provide large logarithms in energy, which are rising with the scattering energy. These contributions cannot be negleted at large energies. One possibility to take this into consideration is a resummation described by the LO BFKL equation [14] which gives an upper bound estimate of these effects.

The Feynman diagrams for A_{QCD} are illustrated in Fig.1. Due to the high-energy factorisation one may calculate first the boson non-forward impact factors Φ associated to the external particles and integrate these with the BFKL Green's function $\mathcal{G}$. The BFKL Green's function is the result of the resummation of leading logarithms in energy, coming from diagrams of ladder topology, built with non-elementary reggeized gluons [14]. The boson impact factor is the convolution of the two boson wave functions which describes the probability that a boson fluctuates into a quark-antiquark pair [15]. The calculation was done for the kinematical region of small scattering angles in the high-energy approximation. Thus, one may neglect terms suppressed by powers of t/s, which simplifies the calculation significantly.

One important property of the helicity flip impact factors need particular attention concerning our further calculations: these impact factors are in general non-zero, they vanish only for forward scattering, where $p_T = 0$. This comes from a different symmetry behaviour of the transverse and longitudinal wave functions. Writing these in a coordinate space formulation [15], the longitudinal wave function is symmetric under the transformation of the dipole size vector $\mathbf{r} \to -\mathbf{r}$, while the transverse one is antisymmetric. Since the dipole interaction is also symmetric under this transformation, the convolution of this with a transverse and longitudinal wave function is antisymmetric, leading to the vanishing result for $p_T = 0$. For non-zero p_T, this symmetry properties are broken, resulting in non-vanishing helicity flip impact factors. Real and imaginary parts of the helicity flip impact factors are oscillating with p_T but shifted in a way that the absolute value of the amplitude gives a smooth function (Fig. 9 of [10]). The helicity flip impact factors are constant in energy, thus the corresponding amplitudes are proportional to the scattering energy s [10, 15]. Because the electroweak parts of the helicity flip amplitude are suppressed by one power of s compared to the QCD ones, the QCD corrections will increase rapidly with energy, leading to significant corrections in the TeV energy regime.

3. The order of magnitude of the QCD corrections is determined in a numerical analysis. Here we consider full circular polarisation of the incoming photons. For the QCD part of the amplitude, due to the huge rapidity separation of the bosons, it is only important if the helicity is conserved or broken in each impact factor. As a result, the amplitude $++ \to TT$

is equal to the amplitude $+- \to TT$ as well as to the amplitude with unpolarised photons. The mass of the Higgs boson was set to $m_H = 115$ GeV unless a different value is stated and the parameters $\alpha_W = \alpha/s_W^2$, $\alpha = 1/128$, $m_Z = 91.2$ GeV, $m_t = 174.3$ GeV and $\alpha_s(M_Z)$ have been used throughout the numerical computations. Since in the QCD expressions [10] the quark masses are always accompanied by the Z mass, they can be negleted in the numerical calculations apart from the top quark mass. The inclusion of the top quark mass reduces the QCD amplitude by 25%.

At high energies in the small angle limit one expects enhancements due to the appearance of large logarithms, these have been resummed in the BFKL scheme. The BFKL resummation was evaluated in the saddle point approximation [10]. The resummed leading log QCD corrections hold an uncertainity resulting from the scale which is not fixed at this order of the calculations. The scale was set to $s_0 = M_Z^2$ in the numerical evaluations. We stress that the resummed leading log QCD corrections at the lower energies we consider, are overshooting what is expected from the true contribution, nevertheless they provide a first estimate of these corrections.

In Fig.2(a-d) QCD corrections to the differential cross sections relative to the pure electorweak contributions are plotted. These relative corrections are defined as:

$$\Delta = \left(\frac{d\sigma_{QCD+EW}}{dp_T^2} - \frac{d\sigma_{EW}}{dp_T^2} \right) \Big/ \frac{d\sigma_{EW}}{dp_T^2} \tag{2}$$

and are presented as functions of p_T^2/M_Z^2 for center of mass energies of 1 Tev and 3 TeV. At these energies $p_T^2/M_Z^2 = 4$ corresponds to values of $\cos\theta$ (where θ is the scattering angle) of 0.90 and 0.99 respectively. Thus, for rising energy the scattering angle will be continously smaller for the same p_T values. For a TESLA detector it was proposed that the tracker system will reach values $\cos\theta < 0.993$, in this range one has a good measurement possibility [16]. Moreover, the decay products of the Z bosons will carry also transverse momenta, thus these particles can have bigger angles from the beam pipe.

Fig.2(a) shows QCD corrections for transverse polarised Z bosons. The electroweak amplitude is mainly imaginary, in agreement with the result of [10] calculated in the high-energy approximation. Therefore, from the QCD amplitude it will be also the imaginary part which mainly accounts for the interference term. The relative corrections are of the order of percent level in the helicity conserving channel. For higher p_T they are approximately one percent and they are rising up to a few percent while approaching the forward region, since the QCD amplitude gets more enhanced compared to the electroweak one. This is due to the fact that in the transition to forward physics the perturbative QCD analysis is increasingly affected by the long distance interactions, since the gluons are massless. The slight rise of the corrections from 1 to 3 TeV is due to the leading log BFKL resummation and is dictated by the Pomeron intercept. Almost at the forward region the imaginary part of the QCD amplitude changes sign and becomes negative which is also visible in the relative corrections.

Next we discuss the helicity breaking cross sections. As discussed in the previous section, the most important property of the helicity flip amplitudes is, that the electroweak parts are not anymore proportional to s as the helicity conserving parts were, so they are supressed by one power of s compared to the QCD part of the amplitude. As a consequence the QCD corrections in comparison to the electroweak part will increase rapidly with the scattering energy, they vanish only for $p_T = 0$. This appear in Fig.2(c) where the relative

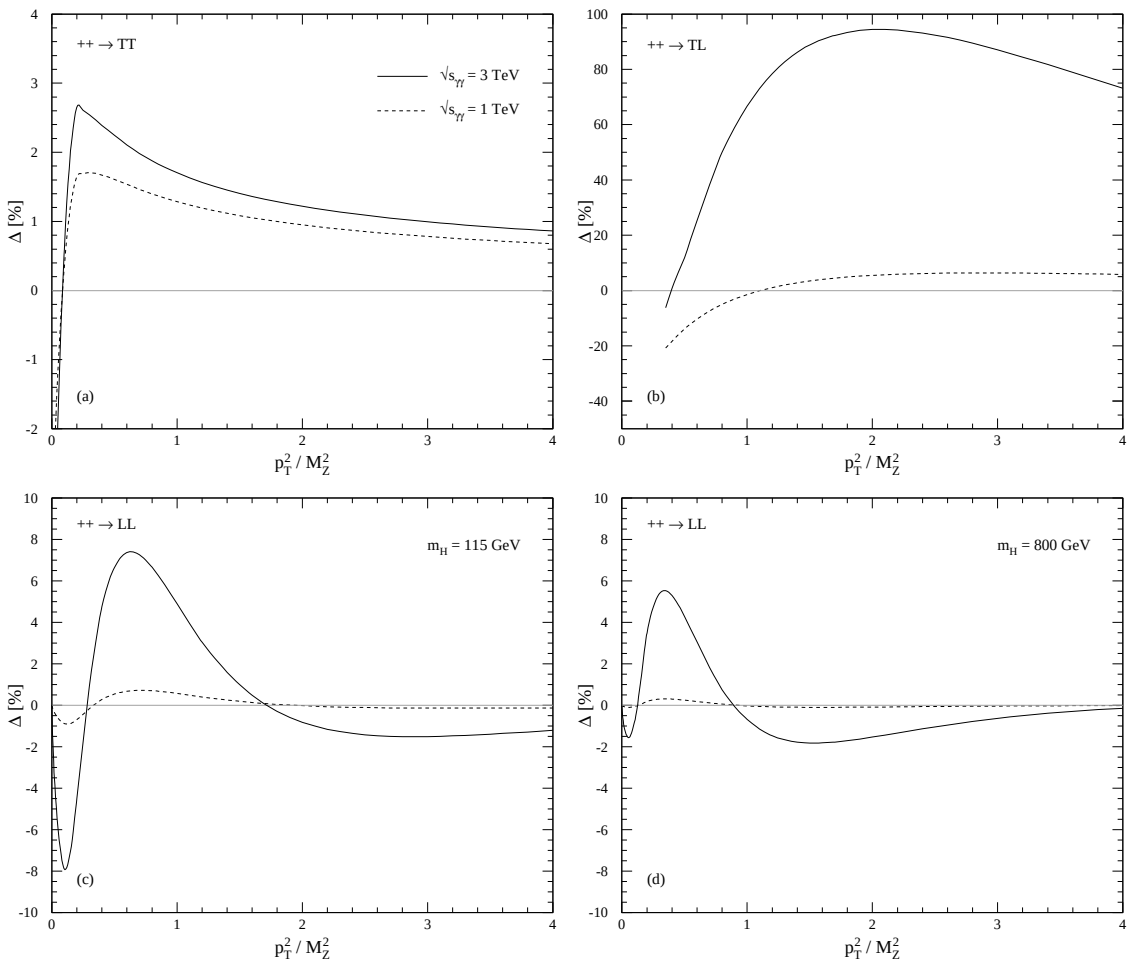

Figure 2: QCD corrections to the differential cross section relative to the pure EW contribution for different Z polarisations and center of mass energies $\sqrt{s}$. The relative correction is defined as $\Delta = (\frac{d\sigma_{QCD+EW}}{dp_T^2} - \frac{d\sigma_{EW}}{dp_T^2}) / \frac{d\sigma_{EW}}{dp_T^2}$.

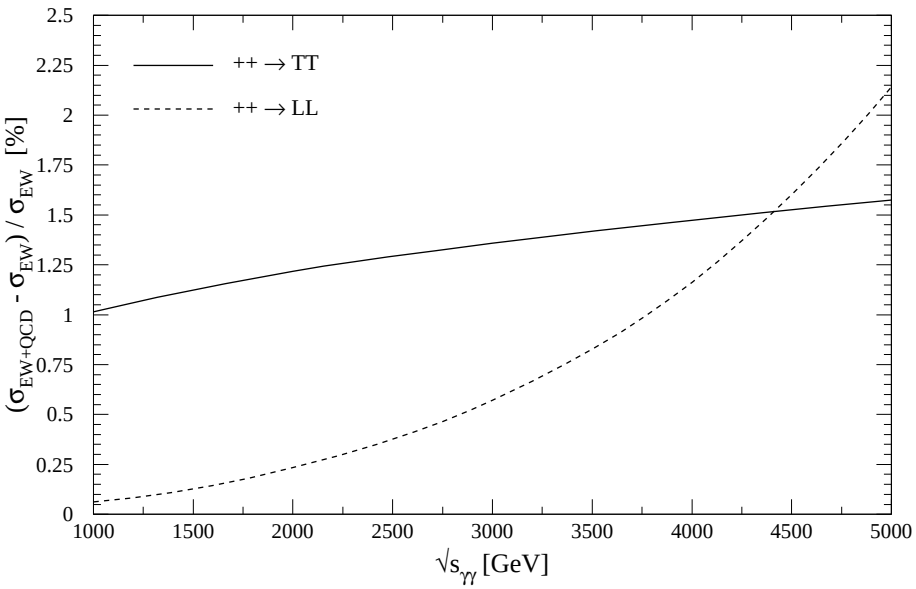

Figure 3: QCD corrections to the integrated cross section relative to the pure EW contribution for transverse and longitudinal polarised Z bosons. The integration region was choosen as $0 < p_T^2 < 4M_Z^2$.

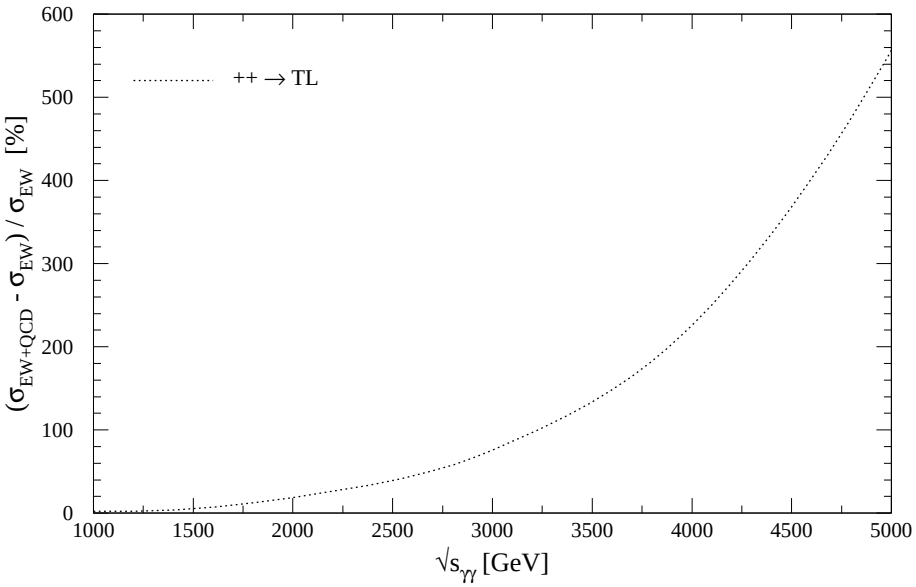

Figure 4: QCD corrections to the integrated cross section relative to the pure EW contribution where the Z bosons have different polarisation. The integration region was choosen as $1/2M_Z^2 < p_T^2 < 4M_Z^2$.

QCD corrections are plotted for longitudinaly polarised Z bosons. The corrections are first rising when p_T is becoming smaller but they vanish for $p_T = 0$. For 1 TeV the corrections are less than 1%, but for 3 TeV they are rising up to 8%. This strong rise is dominating by the different s dependence between the electroweak and QCD amplitude. The additional rise coming from the BFKL resummation is neglible compared to this effect. While the electroweak part of the amplitude was mainly imaginary in the helicity conserving cases, here real and imaginary parts are of the same order. The oscillations visible in the plot are coming entirely from the QCD part of the amplitude, described in the previous section. For higher Higgs masses the real part of the electroweak amplitude gets an enhancement from the Higgs pole contribution, thus the form of the corrections is changing. This is illustrated in Fig.2(d) where the calculation was done for a Higgs mass of $m_H = 800$ GeV.

In Fig.2(b) relative corrections are plotted where one of the Z bosons is transverse and the other longitudinally polarised. The most striking property of these corrections is their magnitude, they can be as high as 100% already at $s = 3$ TeV. This is due to the fact that here the EW part of the amplitude is smaller but the QCD part is bigger in comparison with the case where both Z bosons are longitudinally polarised. The enhancement of the QCD part is coming from the helicity conserving impact factor Φ, which is separated by a huge rapidity gap from the supressed helicity flip impact factor. On the other hand, the QCD part is vanishing for $p_T = 0$ since the helicity flip impact factor does. Because of the dominance of the helicity conserving impact factor, the oscillations coming from the helicity flip impact factor are not visible any more. We observe here again corrections which are rising if p_T gets smaller. Both, electroweak and QCD parts of the amplitude have to vanish for the case of forward scattering due to angular momentum conservation. Since the QCD part has its turning point for bigger p_T, approaching the forward point the corrections are decreasing. We did not plotted corrections up to $p_T = 0$ since eq.(2) lacks of definition at the forward point. Again, here the corrections are rising strongly with s, since the electroweak amplitude is supressed by one power of s compared to the QCD one. The relative corrections are approximately one order of magnitude bigger if s grows from 1 to 3 TeV. The rise resulting from the BFKL resummation is again negligible in this context.

Next we display corrections to the integrated cross section. The high enegy approximation on which the QCD calculation is based, is for a kinematical range where $s \gg -t$. Thus, for the corrections to the integrated cross section we integrated only up to $p_T^2 = 4M_Z^2$, since for high p_T the QCD calculation is loosing its validity. The solid line in Fig.3 displays these corrections for the helicity conserving case. In this integration range the corrections are around one percent and they have a slight rise due to the BFKL resummation, since (up to powers of logarithms) electroweak and QCD amplitudes have the same behaviour in s. The dashed line is for corrections with two longitudinal Z bosons in the final state. In this helicity breaking part the electorweak amplitude is suppressed by one power of s in comparison to the QCD amplitude, so the corrections are rising rapidly with the scattering energy. The smallness of the corrections in the integrated cross section is due to the fact that the corrections to the differential cross section, Fig.2(c), are changing sign with p_T varying, presenting an oscillating behaviour.

In Fig.4 again corrections to the helicity flip cross section are plotted, but here one of the Z bosons is transverse polarised. Due to the different s behaviour of the amplitudes again a strong rise of the corrections with s is present. These are very big, for higher en-

ergies the QCD part of the amplitude completely dominates this part of the cross section. The magnitude of these corrections is mainly due to the helicity conserving impact factor Φ of the QCD amplitude. The integration was done down to $p_T^2 = 1/2M_Z^2$, because the relative corrections lose they meaning for $p_T = 0$, since both amplitudes are vanishing at the forward point.

4. In summary, we have computed QCD corrections for $\gamma\gamma \to ZZ$ at high center of mass energies in the kinematical region of small scattering angles. We have considered the exchange of BFKL gluon ladders which couple to the incoming photons via $\gamma \to Z$ impact factors. The electroweak part was computed in a full one loop calculation, and a complete analysis involving all helicity channels has been done.

In the helicity conserving channel the corrections are at the order of a few percent for $s = O(1\text{ TeV})$ and they show a moderate rise with the scattering energy. In the helicity flip channels the QCD corrections are at the same level for $s = O(1\text{ TeV})$. However, since in this channel the electroweak amplitudes are suppressed by one power of s compared to the QCD ones, the corrections rise much stronger with the scattering energy. Already for $s = O(3\text{ TeV})$ the QCD corrections are significant.

Concerning the QCD corrections we stress, that the leading log BFKL contribution contains a noticable scale dependence. For a more precise analysis one has to use the next-to-leading BFKL Green's function and next-to-leading impact factors. One has also to look in the full SM two loop contribution, in order to achieve precision at the percent level.

On the experimental side the separation of longitudinal and transverse final state Z bosons clearly presents a demanding challenge. Only a statistical analysis of the angular distribution of the decay products of the Z bosons allowes to discriminate between the different polarisations. However, as discussed in the beginning of this letter, a carefull measurement of the process $\gamma\gamma \to ZZ$ with all its different helicity configurations is important and should be persued. The results of our study indicate that in the analysis of the measurements QCD corrections cannot be neglected.

Acknowledgements. We wish to thank J. Bartels for many helpful discussions. The authors are supported by the *Graduiertenkolleg* "Zukünftige Entwicklungen in der Teilchenphysik".

References

[1] G. Jikia, *Nucl. Phys.* **B 405** (1993) 24.

[2] G. Bélanger and F. Boudjema, *Phys. Lett.* **B288** (1992) 210; K. A. Peterson and S. Godfrey, hep-ph/9302297; O. J. P. Éobli, M. C. Gonzaléz-García and S. F. Novaes, *Nucl. Phys.* **B411** (1994) 381; O. J. P. Éobli, M. B. Magro, P. G. Mercandante and S. F. Novaes, *Phys. Rev.* **D52** (1995) 15; S. Godfrey, `hep-ph/9505252`; G. J. Gounaris, F. M. Renard, *Z. Phys.* **C69** (1996) 513; G. J. Gounaris, J. Layssac, F. M. Renard, *Z. Phys.* **C69** (1996) 505; M. Baillargeon, G. Bélanger and F. Boudjema, *Nucl.Phys.* **B500** (1997) 224; E. Boos et al., `hep-ph/0103090`.

[3] I.F. Ginzburg, preprint 28(182) INP Novosobirsk (1990); G.J. Gounaris, J. Layssac, F.M. Renard, *Z. Phys.* **C65** (1995) 505; G.J. Gounaris, F.M. Renard, *Z. Phys.* **C65** (1995) 513; A. T. Banin, I. F. Ginzburg and I. P. Ivanov, *Phys. Rev.* **D59** (1999) 115001.

[4] F. Boudjema, in Physics and Experiments with Linear e^+e^- Colliders, Waikoloa, Hawaii, 1993, Ed. F.A. Harris *et al.*, *Word Sci.*, vol.II, p. 712.

[5] G.J. Gounaris, J. Layssac, P.I. Porfyriadis and F.M. Renard, *Eur. Phys. J.* **C 13** (2000) 79.

[6] J.L. Hewett and F.J. Petriello, *Phys. Rev.* **D64** (2001) 095017.

[7] T. G. Rizzo, *Phys. Rev.* **D60** (1999) 115010; K. Cheung, *Phys. Rev.* **D61** (2000) 015005; H. Davoudiasl, *Phys. Rev.* **D60** (1999) 084022; *Phys. Rev.* **D61** (2000) 044018.

[8] E. E. Boos and G. V. Jikia, *Phys. Lett.* **B275** (1992) 164.

[9] A. Dobado and M.J. Herrero, *Phys. Lett.* **B228** (1989) 495; **233** (1989) 505; J.F. Donoghue and C. Ramirez, *Phys. Lett.* **B234** (1990) 361.

[10] K. Peters and G.P. Vacca `hep-ph/0305137`, *Eur. Phys. J.* **C** (2003) *in press.*

[11] T. Hahn and M. Pérez-Victoria, *Comp. Phys. Commun.* **118** (1999) 153.

[12] J. Küblbeck, M. Böhm, and A. Denner, *Comp. Phys. Commun.* **60** (1990) 165; T. Hahn, `hep-ph/0012260`.

[13] G.J. van Oldenborgh and J.A.M. Vermaseren, *Z. Phys.* **C46** (1990) 425; G.J. van Oldenborgh, *Comp. Phys. Commun.* **66** (1991) 1.

[14] E.A. Kuraev, L.N. Lipatov, V.S.Fadin, *Sov. Phys. JETP* **44** (1976) 443, ibid. **45** (1977) 199, Ya.Ya. Balitskii, L.N. Lipatov, *Sov. J. Nucl. Phys.* **28** (1978) 822.

[15] J. Bartels, K. Golec-Biernat and K. Peters, *Acta Phys. Pol.* **B34** (2003) 3051.

[16] T. Behnke, S. Bertolucci, R. D. Heuer and R. Settles, "TESLA Technical design report. Pt. 4: A detector for TESLA," DESY-01-011